Journal of Power Sources 219 (2012) 100–105

Contents lists available at SciVerse ScienceDirect

Journal of Power Sources

journal homepage: www.elsevier.com/locate/jpowsour

Synthesis and hydrogen storage properties of Mg–La–Al nanoparticles

Tong Liu [a,*], Chenggong Qin [a], Mu Zhu [a], Yurong Cao [a], Hailong Shen [a], Xingguo Li [b,**]

[a] Key Laboratory of Aerospace Materials and Performance (Ministry of Education), School of Materials Science and Engineering, Beihang University, No. 37, Xueyuan Street, Beijing 100191, China

[b] Beijing National Laboratory for Molecular Sciences (BNLMS), The State Key Laboratory of Rare Earth Materials Chemistry and Applications, College of Chemistry and Molecular Engineering, Peking University, Beijing 100871, China

HIGHLIGHTS

- We prepared Mg–La–Al composite nanoparticles by hydrogen plasma–metal reaction.
- These composite nanoparticles can absorb 5.0 wt.% hydrogen in 30 min at 473 K
- The hydrogen absorption activation energy is as low as 23.1 kJ mol^{-1}.
- The LaH_3 nanoparticle and the nanostructured Mg improve the sorption process.

ARTICLE INFO

Article history:
Received 5 April 2012
Received in revised form
3 July 2012
Accepted 11 July 2012
Available online 20 July 2012

Keywords:
Magnesium
Nanoparticles
Hydrogen storage
Kinetics
Crystal structure

ABSTRACT

Mg-2 at.% La-2.6 at.% Al composite nanoparticles are prepared by hydrogen plasma–metal reaction (HPMR) method. The electron microscopy and X-ray diffraction studies reveal that these nanoparticles are made of single crystalline Mg of about 160 nm, and a little amount of polycrystalline Al_2La of 15 nm dispersing on the surface of Mg. The addition of Al effectively reduces the oxidation of Mg nanoparticles. After hydrogenation, Al_2La disproportionates into single crystalline LaH_3 of 15 nm. The composite nanoparticles can absorb 5.0 wt.% H_2 in 30 min even at 473 K, and the storage capacity is as high as 6.8 wt.% at 673 K. They can also release 6.0 wt.% H_2 in less than 10 min at 673 K. The catalytic effect of LaH_3 nanoparticles, nanocrystalline structure and low oxide content of Mg accelerate the hydrogen sorption process of Mg–La–Al composite nanoparticles with a low hydrogen absorption activation energy of 23.1 kJ mol^{-1}.

1. Introduction

Hydrogen is drawing tremendous attentions from both scientists and automotive industry because it is an ideal energy carrier candidate to replace the non-renewable fossil fuels. The development of a safe and efficient hydrogen storage approach is one of the most important issues to realize the hydrogen economy. The conventional hydrogen storage methods through the compressed hydrogen gas and the cryogenic hydrogen liquid cannot meet the requirements of the on-board applications due to the problems of low hydrogen storage capacity, unsafe and high cost. It is known that hydrogen storages via solid state materials have the potential advantages of high storage capacity and safety [1]. So far, many kinds of hydrogen storage materials have been developed, including $LaNi_5$ [2], Mg_2Ni [3], alanates [4], amides [5], carbon nanotubes [6] and metal-organic frameworks [7]. Among the metal hydrides, MgH_2 is still the most attractive one because of its high theoretical gravimetric capacity of 7.6 wt.%, abundance and low cost. Nevertheless, up to now, the commercial application of MgH_2 has not been fully achieved as the result of its slow hydrogen sorption kinetics and high operational temperature [8].

In recent years, the addition of catalysts has been considered as one of the effective approaches to improve the hydrogen sorption kinetics of Mg hydride. Among alloying elements, Al is known as one of the most attractive candidates to decrease the stability of magnesium hydride [9–12]. The Mg–Al binary system contains several stable intermetallic phases, such as β-Mg_2Al_3, R–$Mg_{42}Al_{58}$ and γ-$Mg_{17}Al_{12}$ [13], whose hydrogen storage capacities are 3.02, 3.17 and 4.44 wt.%, respectively [14]. It has been observed that the

* Corresponding author. Tel.: +86 10 8231 6192; fax: +86 10 8231 4869.
** Corresponding author. Tel.: +86 10 6275 3691; fax: +86 10 6276 5930.
E-mail addresses: tongliu@buaa.edu.cn (T. Liu), xgli@pku.edu.cn (X. Li).

0378-7753/$ – see front matter © 2012 Elsevier B.V. All rights reserved.
http://dx.doi.org/10.1016/j.jpowsour.2012.07.027

Table 1
ICP results of the as-prepared Mg–La–Al nanoparticles.

	ICP measurement ($\mu g\ ml^{-1}$)				Concentration of elements in the nanoparticle (at.%)
	Test 1	Test 2	Test 3	Average	
Mg	27.7	27.7	27.9	27.8	95.4
La	3.35	3.35	3.36	3.35	2.0
Al	0.818	0.833	0.830	0.827	2.6

hydrogen sorption kinetics of Mg was significantly improved with Al addition, and the enthalpy of hydrogenation was decreased upon alloying with Al as the result of the endothermic disproportionation reactions of Mg–Al intermetallic compounds [14,15]. Crivello et al. reported that $Mg_{75}Al_{25}$ alloy can absorb nearly 5 wt.% H_2 at 623 K, but the hydrogenation kinetics below 573 K are still too slow for practical application [16]. On the other hand, it has been reported that the addition of rare earth elements is able to effectively enhance the hydrogen storage properties of Mg [17–19]. La_2Mg_{17} is able to absorb about 6 wt.% H_2 at 623 K [17]. Ouyang and coworkers observed that Mg_3La alloy can absorb hydrogen even at room temperature and the maximum hydrogen absorption capacity is 2.89 wt.% at 570 K [18]. Guo and Huang found that the increase of La addition was favorable to decrease hysteresis of hydrogen absorption/desorption in La–Mg–Ni alloys [19]. Although both Al and La are able to improve the hydrogen sorption of Mg, the combining effects of Al and La on the hydrogen storage properties of Mg are still rarely reported.

High energy ball milling (HEBM) has been adopted not only to produce the nanostructured hydride particles, but also to disperse the catalysts effectively [20–24]. However, the processing of HEBM usually takes a long time, and it is difficult to prevent the particles from oxidation and contamination by milling media during the milling process. Moreover, it is hard for HEBM to reduce the particle sizes of metals/hydrides to nano-scale. HPMR method is a novel vapor deposition processing and suitable for producing metallic nanoparticles industrially with high purity and low cost. Up to now, nanoparticles of several alloys and intermetallics have been fabricated by using HPMR approach, and the particle size can be tuned by controlling the hydrogen pressure and the current value [25–27]. In this work, we intend to fabricate the Mg–La–Al composite nanoparticles using HPMR method, investigate the synergic effects of La and Al on the hydrogen sorption properties, and study the phase transformations during the hydrogen absorption and desorption cycle.

2. Experimental

The equipment for producing nanoparticles primarily contained an arc melting chamber and a collecting system, which was described elsewhere [25]. Firstly, Mg, Al and La (purity > 99.5%) with a mole ratio of 8:1:1 were melted in the induction furnace. The $Mg_{80}Al_{10}La_{10}$ ingot of 20 g was put in the reaction chamber. The Mg–La–Al nanoparticles were produced by arc melting the ingot in a 50% Ar and 50% H_2 mixture of 0.1 MPa. The flow rate of the circulation gas for the collection of nanoparticles was 100 L min^{-1}. The arc current was selected as 80 A. Before the nanoparticles were taken out from the collection room, they were passivated with a mixture of argon and air.

The hydrogen absorption and desorption properties of the as-prepared Mg–La–Al nanoparticles were evaluated using a Sieverts-type apparatus. The volume of the reactor chamber was about 60 ml, and the error of the measurement was less than 5%. After the Mg–La–Al nanoparticles of 100 mg were put into the Sieverts reactor, the system was evacuated to 10^{-3} Pa. Then, the samples were heated up to 423, 473, 523, 573, 623 and 673 K, respectively. A hydrogen pressure of 4 MPa (purity > 99.999%; N_2 < 5.0, O_2 < 2.0 and H_2O < 2.0 ppm) was provided to make the Mg–La–Al nanoparticles absorb hydrogen to measure the absorption kinetic curves. The desorption kinetic curves at various temperatures were measured at an initial pressure of about 100 Pa by evacuating the system. A conventional pressure–volume–temperature technique was used to obtain the hydrogen sorption curves and pressure–composition isotherm (*P–C–T*) curves of the Mg–La–Al nanoparticles at 623, 648 and 673 K. Once the change of hydrogen pressure was less than 20 Pa per second, the hydrogen absorption or desorption process at certain pressure during the *P–C* isotherm measurement was considered as reaching an equilibrium.

The chemical composition of the nanoparticle sample was determined by the induction-coupled plasma (ICP) spectroscopy. The structural analysis of the Mg–La–Al nanoparticle samples before and after the hydrogen sorption were carried out by X-ray diffraction (XRD) using a Rigaku X-ray diffractometer with monochromatic Cu Kα radiation. The morphology, size distribution and shape of the nanoparticle samples before and after the hydrogen

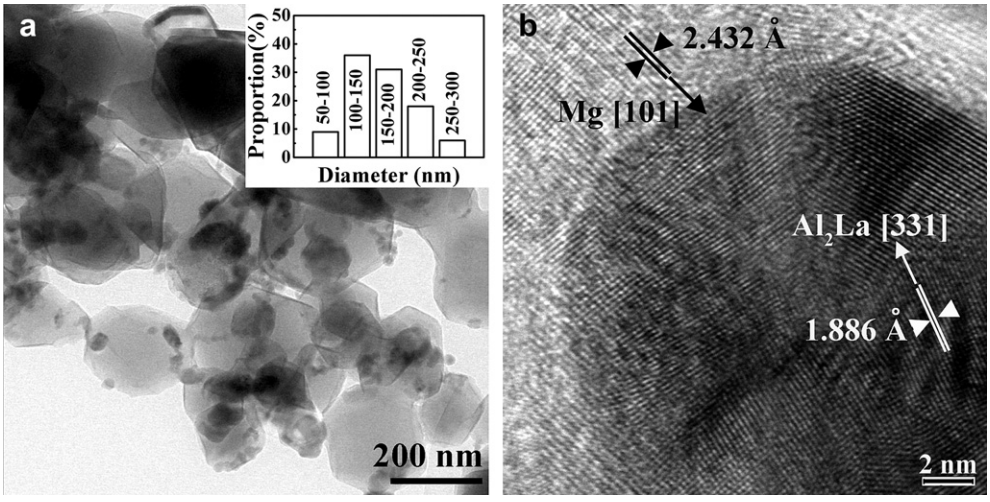

Fig. 1. TEM bright-field image of the as-prepared Mg–La–Al nanoparticles (a) and HR-TEM image of one Mg–La–Al nanoparticle (b).

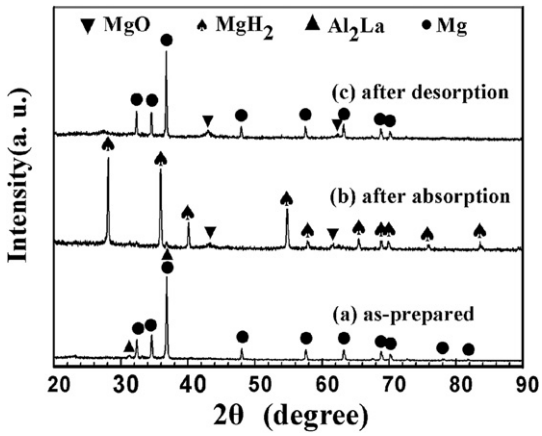

Fig. 2. X-ray diffraction patterns of the Mg–La–Al nanoparticles (a) as-prepared, (b) after the absorption under 4 MPa hydrogen pressure at 673 K, and (c) after the hydrogen desorption under 100 Pa at 673 K.

sorption were observed by TEM using JEOL-JSM-2100 at an accelerating voltage of 200 kV.

3. Results and discussion

3.1. Particle features

Table 1 shows the chemical composition of the as-prepared nanoparticle sample evaluated by ICP spectroscopy. It can be seen that for the master alloy containing 80 at.% Mg, 10 at.% La and 10 at.% Al, there are 95.4 at.% Mg, 2 at.% La and 2.6 at.% Al in the as-prepared nanoparticle sample. It should be noted that the higher Mg content in the as-prepared nanoparticles than that in the master ingot is attributed to the lower evaporation enthalpy of Mg (127.4 kJ mol^{-1}) than those of Al (414 kJ mol^{-1}) and La (402 kJ mol^{-1}) [28]. Fig. 1a displays the TEM image of the as-prepared Mg–La–Al nanoparticles. It is apparently observed that there are two kinds of particles. The big particles have clear hexagonal shapes, which are the same as the pure Mg nanoparticles prepared by HPMR [29]. They vary from 50 to 250 nm with an average size of about 160 nm. On the surface of each big particle, many fine particles of about 15 nm in nearly spherical shape are dispersed. Fig. 1b shows the high-resolution TEM (HR-TEM) image of the Mg–La–Al composite nanoparticle. The lattice fringes are clearly seen in the big particle and the measured lattice spacing is 2.432 Å, which corresponds to the hcp-Mg (101) plane, indicating that the big particle is Mg with a single crystal structure. It is interesting to observe that the small particle belongs to poly-crystalline structure. One lattice spacing is evaluated to be 1.886 Å in Fig. 1b for the small particle, which corresponds to the (331) plane of Al_2La. The crystal structure of the nanoparticle sample is also supported by the XRD result discussed hereafter.

Fig. 2 shows the XRD patterns of the as-prepared nanoparticles and the samples obtained after the hydrogen absorption and desorption at 673 K. It is found in Fig. 2a that the as-prepared sample is composed dominantly of α-Mg (hcp) structure and a little amount of Al_2La, in excellent agreement with the TEM observation. The lattice constants of Mg calculated from the XRD data are $a = 3.201$ Å and $c = 5.201$ Å, slightly lower than the standard data of α-Mg (PDF35-0821, $a = 3.209$ Å, $c = 5.211$ Å). This indicates that Al with smaller metallic radii (143 pm) than Mg (160 pm) partially dissolves in the hcp-Mg and decreases the lattice constant [30]. This agrees with the Mg–Al and Mg–La binary diagrams that La and Mg are immiscible, and Al has a certain solutability in Mg [31]. Mg ultrafine particles are usually very reactive toward oxygen [32]. Surface modification is an effective way to protect Mg from being oxidized. Recently, Mg composite nanoparticles have been embedded in a gas-selective polymer matrix, which made them air-stable [33]. However, the hydrogen storage capacity of these particles was decreased to 4 wt% due to the high matrix polymer content of about 40 wt%. Krishnan and co-workers endeavored to cover Mg ultrafine particles with metallic layer by inert gas condensation technique [34]. They produced the Mg–Ti nanoparticles by magnetron sputtering in an inert Kr atmosphere. However, it was found that the Mg and Ti nanoparticles were covered with MgO shell of 3–4 nm in thickness. It is worth to note that the diffraction peak of MgO around 42.9°, which often appears in the Mg particles prepared by HPMR [28], cannot be detected in the present XRD pattern. MgO shell is not discernable in the TEM observation as well. It can be concluded that the addition of Al and La effectively suppressed the oxidation tendency of Mg, leading to the decrease of MgO content in the nanoparticles after passivation. Due to the high oxidation resistance of Al, it is proposed that Al plays more important role than La in preventing Mg from oxidation. From the XRD pattern in Fig. 2b, it can be found that after the

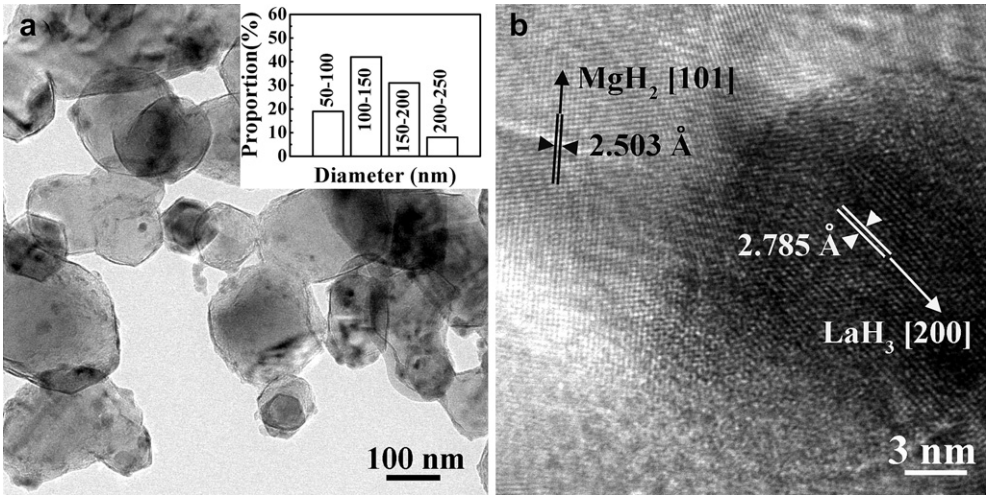

Fig. 3. TEM bright-field image of the Mg–La–Al nanoparticles after the hydrogen absorption (a) and HR-TEM image of one Mg–La–Al nanoparticle after the hydrogenation (b).

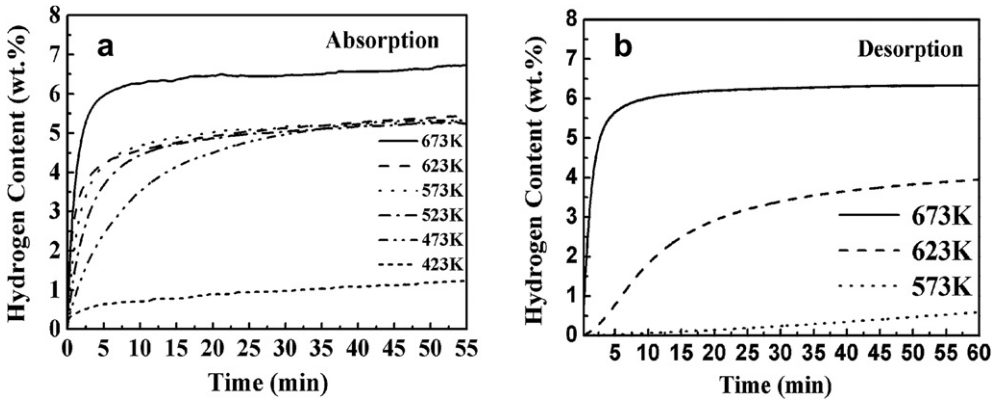

Fig. 4. Hydrogen absorption curves of the Mg–La–Al nanoparticles at 423, 473, 523, 573, 623 and 673 K under 4 MPa hydrogen pressure (a) and the desorption curves at 573, 623 and 673 K (b).

hydrogen absorption process at 673 K, Mg nanoparticles transforms into MgH_2. However, La hydride is not detected from the XRD pattern, probably due to its low concentration. It is observed from Fig. 2c that after the hydrogen desorption at 673 K, MgH_2 decomposes completely and α-Mg is recovered. According to the previous study, LaH_3 will not release hydrogen in present condition [17]. It is proposed that these LaH_3 nanoparticles are crucial to catalyze the hydrogenation of Mg. We can also detect MgO in Fig. 2b and c, which is attributed to the fact that after the absorption and desorption processes the nanoparticles were taken out of the chamber without passivation.

Fig. 3a shows the TEM image of Mg–La–Al nanoparticles after the hydrogenation. It is interesting to find that after the hydrogen absorption, the MgH_2 nanoparticles are no longer of hexagonal shape but change into quasi-spherical shape with an average size of about 140 nm. It is also discernable from Fig. 3a that the fine black dots known as LaH_3 nanoparticles of about 15 nm are distributed on the surface of MgH_2. Fig. 3b shows the HR-TEM image of the Mg–La–Al nanoparticle after the hydrogenation. The lattice fringes are clearly seen in the big particle matrix and the measured lattice spacing is 2.503 Å, which corresponds to the MgH_2 (101) plane. The lattice spacing of the small particle is evaluated to be 2.785 Å, which corresponds to the (311) plane of LaH_3, implying that the small particle belongs to single crystal LaH_3. These phases determined from the HR-TEM analyses are in well agreement with the XRD results.

On the basis of the analysis above, the formation of Mg–La–Al composite nanoparticles by HPMR and the hydrogen absorption and desorption processes can be summarized into the following equations, respectively:

$$Mg + La + Al \rightarrow Mg + Al_2La \quad (1)$$

$$Mg + Al_2La + H_2 \rightarrow MgH_2 + LaH_3 + Al \quad (2)$$

$$MgH_2 + LaH_3 + Al \rightarrow Mg(Al) + LaH_3 + H_2 \quad (3)$$

3.2. Hydrogen storage properties

The activation treatment through annealing at 673 K in vacuum and in hydrogen for several cycles is often required for the micro-size Mg particles. However, even after this activation process, Mg at microscale could absorb only 1.5 wt.% H_2 within 2 h at a temperature as high as 673 K [8]. Fig. 4a shows the hydrogen absorption curve of the Mg–La–Al composite nanoparticles at different temperatures. It can be observed that these composite nanoparticles can absorb 1.3 wt.% H_2 at 423 K. The hydrogen absorption rate increases with increasing the temperature from 423 to 673 K. They can absorb 5.0 wt.% H_2 in less than 30 min at 473 K, quite faster than the micro-sized Mg. Compared with many catalyzed Mg particles, the Mg–La–Al composite nanoparticles also show superior hydrogen absorption performance [21–23,35–38]. For example, the nanocrystalline Mg–Ni–La alloy derived from the corresponding amorphous alloy had a hydrogen storage capacity of 4.6 wt.% at 513 K [38], which is lower than that of the Mg–La–Al composite nanoparticles. It is also observed in

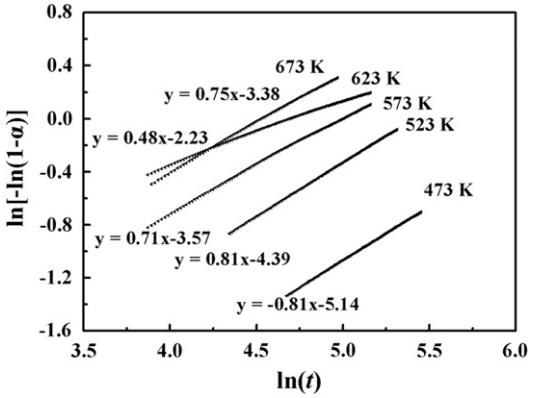

Fig. 5. Plot $\ln(-\ln(1-\alpha))$ vs. $\ln(t)$ for the hydrogenation of the Mg–La–Al nanoparticles.

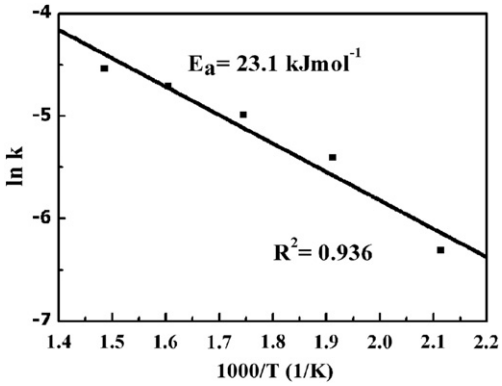

Fig. 6. Absorption plot of ln k vs. 1000/T of the Mg–La–Al nanoparticles.

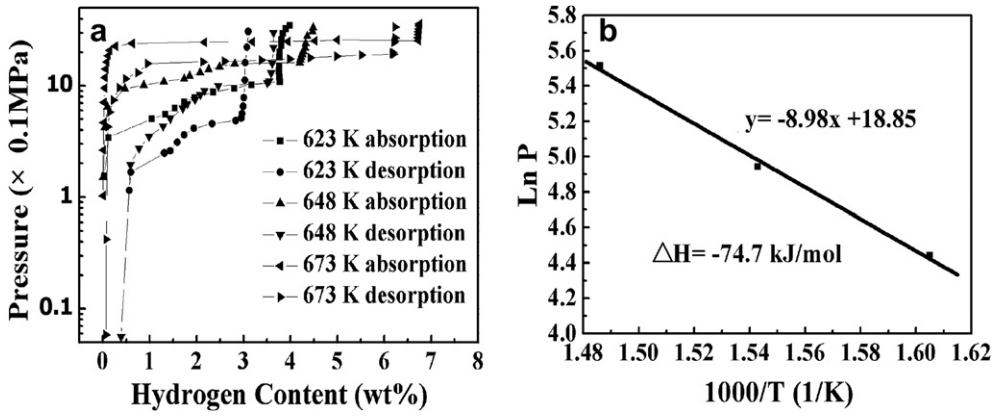

Fig. 7. Pressure–composition isotherm curves of the Mg–La–Al nanoparticles at 623, 648 and 673 K (a) and Van't Hoff plot for the Mg–La–Al nanoparticles (b).

Fig. 4a that at 523, 573, 623, and 673 K, the hydrogen absorption content enlarges remarkably with time in the initial absorption stage and reaches a value of 4.4, 4.6, 4.8 and 6.3 wt.% in 10 min, respectively. It was reported that the maximum hydrogen absorption capacity of Mg_3La alloy is 2.89 wt.% at 570 K [18], and the $Mg_{75}Al_{25}$ compound can absorb nearly 5 wt.% H_2 at 623 K [16]. In this work, the Mg–La–Al composite nanoparticles can uptake 5.3 wt.% H_2 at 573 K, showing a superior hydrogen storage property. Fig. 4b shows the hydrogen desorption curve of the Mg–La–Al nanoparticles at different temperatures. It can be seen that the hydrogen desorption content enlarges remarkably with the increasing temperature in the initial desorption stage and reaches a value of 6.0 wt.% in 10 min at 673 K with a saturation value of 6.3 wt.%. At 623 K, the Mg–La–Al nanoparticles can dehydrogenate nearly 4.0 wt.% H_2, displaying improved sorption kinetics.

The activation energy for hydrogen absorption is usually calculated from the JMAK (Johnson–Mehl–Avrami–Kolmogorov) model and the Arrhenius theory. On the basis of JMAK model, the hydrogen absorption kinetics can be expressed in the following linear equation:

$$\ln[-\ln(1-\alpha)] = \eta \ln k + \eta \ln t \quad (4)$$

where α is the fraction transformed at time t, k is an effective kinetic parameter, η is the Avrami exponent of reaction order. For the experimental data of 473, 523, 573, 623 and 673 K, by plotting ln $[-\ln(1-\alpha)]$ vs. ln(t) shown in Fig. 5, each temperature provides a straight line with a slope η and an intercept $\eta \ln(k)$. After calculating the rate constant k from the η value, the apparent activation energy for the absorption process is evaluated from the Arrhenius equation:

$$K = A \cdot \exp(E_a/RT) \quad (5)$$

where A is a temperature-independent coefficient, E_a is the apparent activation energy, R is the gas constant (8.314 J mol^{-1} K^{-1}), and T is the absolute temperature. The absorption plot of ln(k) vs. 1000/T is shown in Fig. 6. It is found that the fit (R^2) is 0.936, implying that the experimental data can be evaluated by JMAK model and Arrhenius theory. The calculated hydrogen absorption activation energy of the Mg–La–Al nanoparticles is 23.1 kJ mol^{-1}, which is far lower than those of the micro-sized Mg particles and many catalyzed Mg particles [21–23,35–37].

Fig. 7a shows the P–C–T curves of the hydrogen absorption-desorption for the Mg–La–Al nanoparticles at 623, 648 and 673 K. The hydrogen pressures of the absorption plateaus are 2.47 MPa at 673 K, 1.40 MPa at 648 K and 0.85 MPa at 623 K. From these data, the Van't Hoff Plot (ln P vs. T^{-1}) for the hydrogen absorption of the Mg–La–Al nanoparticles is built in Fig. 6b. According to the fitting line from the experimental data, the Van't Hoff equation for the absorption is $\ln(P) = -8.98/T + 18.85$. The obtained value of the formation enthalpy (ΔH) for the Mg–La–Al composite nanoparticles is −74.7 kJ mol^{-1}, similar with the formation enthalpy for Mg particles reported by other works [39,40]. This implies that a small addition of La and Al to Mg does not apparently alter the thermodynamics of the hydrogenation process.

It is well known that the hydrogenation rate of Mg is affected by several factors.

Firstly, the surface of pure magnesium without catalytic additives requires a very high energy for the dissociation of H_2. In the present work, the LaH_3 nanoparticles dispersed on the surface of Mg particles act as a catalyst to decrease the dissociation energy of H_2 and improve the hydrogen sorption kinetics of Mg. Secondly, the formation rate of MgH_2 on the Mg surface and along the grain boundaries are the critical factors to impact the hydrogenation capacity and kinetics, because the diffusion coefficient of hydrogen in MgH_2 is much smaller than that in Mg [41]. It was also reported that the hydrogenation rate of the magnesium decreased with increasing the hydride layer thickness [42]. When the thickness of hydride layer exceeded 30–50 μm, the hydrogenation reaction stopped abruptly [8,43]. In this work, the fine particle size decreases the thickness of MgH_2, and the nano-sized grain accelerates the hydrogen diffusion, resulting in the improved hydrogen sorption kinetics of Mg particles. Additionally, it is known that the oxide layer of Mg particles prevents hydrogen from transporting into Mg. In this work, the decrease of oxide content due to the addition of Al accelerates the sorption of hydrogen on the surface of Mg particles. Thus, the high hydrogen sorption rate and storage capacity with a very low hydrogen absorption activation energy is attributed to the combined effects of the catalytic LaH_3 nanoparticles, the decreased oxide content and the fine particle/grain size. The Mg–La–Al composite nanoparticles with high sorption kinetics, high storage capacity, and low hydrogenation temperature, are a promising candidate for hydrogen storage.

4. Conclusions

The Mg-2 at.% La-2.6 at.% Al composite nanoparticles were prepared from the $Mg_{80}La_{10}Al_{10}$ ingot by HPMR method. These nanoparticles were made of Mg and a little amount of Al_2La. Mg nanoparticles of single crystalline were polyhedron in shape, varying from 50 to 250 nm with an average size of about 160 nm, The polycrystalline Al_2La nanoparticles of spherical shape had a mean diameter of 15 nm, dispersing on the surface of Mg

nanoparticles. The addition of Al effectively reduced the oxidation of Mg nanoparticles. After hydrogenation, the mean particle size of MgH_2 nanoparticles was 140 nm, and Al_2La disproportionated into single crystalline LaH_3 of 15 nm, dispersing on the surface of MgH_2.

The addition of La and Al played a crucial role in enhancing the sorption kinetics properties of the Mg–La–Al nanoparticles. After one sorption cycle for the activation, these nanoparticles can absorb hydrogen even at 473 K and reach a value of 5.0 wt.% in 30 min. Moreover, they can absorb 6.3 wt.% H_2 in less than 10 min at 673 K. It can also release 6.0 wt.% H_2 in 10 min at 673 K. The catalytic effect of LaH_3 nanoparticles, nanocrystalline structure and low oxide content of Mg nanoparticles promoted the hydrogen sorption process with a low hydrogen absorption activation energy of 23.1 kJ mol^{-1}. The enhanced hydrogen sorption kinetics and high storage capacity were due to the improved kinetics rather than the change in enthalpy.

Acknowledgments

The authors acknowledge the support of this work by MOST of China (No. 2011AA03A408), the Aeronautical Science Foundation of China (No. 2011ZF51065), the Fundamental Research Funds for the Central Universities (No. YWF1102212), and the Specialized Research Fund for the Doctoral Program of Higher Education (No. 20091102120009).

References

[1] B. Sakintuna, F. Lamari-Darkrim, M. Hirscher, Int. J. Hydrogen Energy 32 (2007) 1121–1140.
[2] A. Demircan, M. Demiralp, Y. Kaplan, M.D. Mat, T.N. Veziroglu, Int. J. Hydrogen Energy 30 (2005) 1437–1446.
[3] C.A. Chung, C.S. Lin, Int. J. Hydrogen Energy 34 (2009) 9409–9423.
[4] S.I. Orimo, Y. Nakamori, J.R. Eliseo, A. Züttel, C.M. Jensen, Chem. Rev. 107 (2007) 4111–4132.
[5] H.Y. Leng, T. Ichikawa, S. Hino, N. Hanada, S. Isobe, H. Fujii, J. Power Sources 156 (2006) 166–170.
[6] Y.L. Kuan, T.T. Wen, J.Y. Tsong, J. Power Sources 196 (2011) 3389–3394.
[7] J.L.C. Rowsell, O.M. Yaghi, Angew. Chem. Int. Ed. 44 (2005) 4670–4679.
[8] A. Zaluska, L. Zaluski, J.O. Strom-Olsen, J. Alloys Compd. 288 (1999) 217–225.
[9] A. Zaluska, L. Zaluski, J.O. Strom-Olsen, Appl. Phys. A 72 (2001) 157–165.
[10] C.X. Shang, M. Bououdina, Z.X. Guo, Mater. Trans. 44 (2003) 2356–2362.
[11] A. Andreasen, M.B. Sorensen, R. Burkarl, B. Moller, J. Alloys Compd. 404 (2005) 323–326.
[12] S. Bouaricha, J.P. Dodelet, D. Guay, J. Huot, S. Boily, R. Schulz, J. Alloys Compd. 297 (2000) 282–293.
[13] J.L. Murray, J. Phase Equilib. Diff. 3 (1982) 60–74.
[14] A. Andreasen, Int. J. Hydrogen Energy 33 (2008) 7489–7497.
[15] A.S. El-Amoush, J. Alloys Compd. 441 (2007) 278–283.
[16] J.C. Crivello, T. Nobuki, T. Kujic, Int. J. Hydrogen Energy 34 (2009) 1937–1943.
[17] S. Yajima, J. Kayano, H. Toma, J. Less Common Met. 55 (1977) 139–141.
[18] L.Z. Ouyang, F.X. Qin, M. Zhu, Scr. Mater. 55 (2006) 1075–1078.
[19] J. Guo, D. Huang, Mater. Sci. Eng. B 131 (2006) 169–172.
[20] N. Hanada, T. Ichikawa, H. Fujii, J. Phys. Chem. B 109 (2005) 7188–7194.
[21] M.Y. Song, J.L. Bobet, B. Darriet, J. Alloys Compd. 340 (2002) 256–262.
[22] G. Liang, J. Huot, S. Boily, A. Van Neste, R. Schulz, J. Alloys Compd. 292 (1999) 247–252.
[23] R.L. Holtz, M.A. Imam, J. Mater. Sci. 34 (1999) 2655–2663.
[24] J. Lu, Y.J. Choi, Z.Z. Fang, H.Y. Sohn, E. Ronnebro, J. Am. Chem. Soc. 131 (2009) 15843–15852.
[25] T. Liu, T.W. Zhang, M. Zhu, C.G. Qin, J. Nanopart. Res. 14 (2012) 738–745.
[26] T. Liu, H.Y. Shao, X.G. Li, Intermetallics 12 (2004) 97–102.
[27] T. Liu, H.Y. Shao, X.G. Li, Nanotechnology 14 (2003) 542–545.
[28] H.K. Kugler, C. Keller, Gmelin Handbook of Inorganic and Organometallic Chemistry, eighth ed., Springer-Verlag, Berlin, 1985.
[29] T. Liu, Y.H. Zhang, X.G. Li, Scr. Mater. 48 (2003) 397–402.
[30] N.N. Greenwood, A. Earnshaw, Chemistry of the Elements, second ed., Butterworth-Heinemann, Oxford, 1997.
[31] B.M. Thaddeus, L.M. Joanne, H.B. Lawrence, B. Hugh, K. Linda, Am. Soc. Met. (1986).
[32] A. Chaise, P. de Rango, P. Marty, D. Fruchart, Int. J. Hydrogen Energy 35 (2010) 6311–6322.
[33] K.J. Jeon, H.R. Moon, A.M. Ruminski, B. Jiang, C. Kisielowski, R. Bardhan, J.J. Urban, Nat. Mater. 10 (2011) 286–290.
[34] G. Krishnan, G. Palasantzas, B. Kooi, J. Appl. Phys. Lett. 97 (2010) 261912.
[35] T.R. Jensen, A. Andreasen, T. Vegge, J.W. Andreasen, K. Ståhl, A.S. Pedersen, M.M. Nielsen, A.M. Molenbroek, F. Besenbacher, Int. J. Hydrogen Energy 31 (2006) 2052–2062.
[36] T. Liu, T.W. Zhang, X.Z. Zhang, X.G. Li, Int. J. Hydrogen Energy 36 (2011) 3515–3520.
[37] T. Liu, T.W. Zhang, C.G. Qin, M. Zhu, X.G. Li, J. Power Sources 196 (2011) 9599–9604.
[38] K. Tanaka, J. Alloys Compd. 450 (2008) 432–439.
[39] J.F. Stampfer, C.E. Holley, J.F. Suttle, J. Am. Chem. Soc. 82 (1960) 3504–3508.
[40] W. Klose, V. Stuke, Int. J. Hydrogen Energy 20 (1995) 309–316.
[41] D.S. Sholl, J. Alloys Compd. 446 (2007) 462–468.
[42] X. Yao, Z.H. Zhu, H.M. Cheng, G.Q. Lu, J. Mater. Res. 23 (2008) 336–340.
[43] B. Vigeholm, J. Kjoller, B. Larsen, A.S. Pedersen, J. Less Common Met. 89 (1983) 135–144.